



The Compact Muon Solenoid Experiment  
**Conference Report**

Mailing address: CMS CERN, CH-1211 GENEVA 23, Switzerland



25 July 2010 (v2, 29 July 2010)

# Measurement of the muon stopping power in lead tungstate with the Electromagnetic Calorimeter in CMS

Andrea Davide Benaglia on behalf of the CMS Collaboration

## Abstract

A large sample of cosmic ray events collected by the CMS detector has been exploited to measure the muon stopping power in the lead tungstate ( $\text{PbWO}_4$ ) of the electromagnetic calorimeter. The events were recorded in October-November 2008, during commissioning runs of the CMS detector with the solenoid at the nominal field strength of 3.8 T. The measurement spans a momentum range from 5 to 1000 GeV/c. The results are consistent with the expectations over the entire range. A comparison of collision losses with radiative losses allowed for a first experimental determination of muon critical energy in lead tungstate, measured to be  $160_{-6}^{+5}$  (stat.)  $\pm 8$  (syst.) GeV, in agreement with expectations.

Presented at *CALOR2010: 14th International Conference for Calorimetry in High Energy Physics*

# Measurement of the Muon Stopping Power in Lead Tungstate with the Electromagnetic Calorimeter in CMS

A D Benaglia<sup>1</sup> on behalf of the CMS Collaboration

<sup>1</sup> Università degli Studi di Milano - Bicocca and INFN - Piazza della Scienza 3, Milano, Italy

E-mail: [andrea.benaglia@mib.infn.it](mailto:andrea.benaglia@mib.infn.it)

**Abstract.** A large sample of cosmic ray events collected by the CMS detector has been exploited to measure the muon stopping power in the lead tungstate (PbWO<sub>4</sub>) of the electromagnetic calorimeter. The events were recorded in October-November 2008, during commissioning runs of the CMS detector with the solenoid at the nominal field strength of 3.8 T. The measurement spans a momentum range from 5 to 1000 GeV/c. The results are consistent with the expectations over the entire range. A comparison of collision losses with radiative losses allowed for a first experimental determination of muon critical energy in lead tungstate, measured to be  $160_{-6}^{+5}$  (stat.)  $\pm 8$  (syst.) GeV, in agreement with expectations.

## 1. Introduction

During the commissioning phase conducted with cosmic ray events [1], the electromagnetic calorimeter (ECAL) of the Compact Muon Solenoid (CMS) experiment has been exploited to measure the muon stopping power in the lead tungstate of its crystals.

The stopping power for muons in the energy range considered can be conveniently written as

$$f(E) = \left\langle -\frac{dE}{dx} \right\rangle = a(E) + b(E)E,$$

where  $E$  is the total muon energy,  $x$  is the thickness of the traversed material, commonly measured in mass per unit surface,  $a(E)$  is the stopping power due to collisions with atomic electrons, and  $b(E)$  is due to radiative processes: bremsstrahlung, direct pair production, and photonuclear interactions;  $a(E)$  and  $b(E)$  are slowly varying functions of  $E$  at energies where radiative contributions are important [2, 3].

Numerical values of stopping power and related quantities quoted throughout this report are taken from tables in [4, 5]. The theoretical uncertainties are everywhere smaller than the statistical precision of the results in this analysis.

The definition of critical energy as the energy at which the average rates of energy loss through collision and radiation are equal [2, 3] is adopted here. Analysis of data in the full momentum range permits a comparison of collision losses with radiative losses, thus leading to the first experimental determination of muon critical energy.

See [6] for a detailed description of the CMS detector.

## 2. Measurement of physical variables and event selection

The physical variables to be measured for each muon are the momentum ( $p$ ), the path length in ECAL ( $\Delta x$ ), and the energy lost in ECAL ( $\Delta E$ ) [7].

The muon momentum is measured from the track fit performed in the inner tracking system [8].

The path length in ECAL is estimated by propagating the measured muon track inside the calorimeter taking into account bending due to the magnetic field and expected energy loss. The average path length in ECAL for the selected muon sample is 22.0 cm, from which it follows that the typical energy loss for a minimum ionizing muon is about 300 MeV.

The energy deposited in ECAL barrel<sup>1</sup> by cosmic ray muons is measured by means of a dedicated algorithm. Online data reduction is based on zero suppression (ZS), that is, a readout of channels above a ZS threshold of about 20 MeV, and on a full readout of selected regions (SR) of high interest, with a threshold set to about 170 MeV [9]. When the condition for SR is met, a matrix of  $3 \times 3$  trigger towers is read out. Each tower is comprised of  $5 \times 5$  crystals and the matrix is centered around the tower with energy deposit above the SR threshold.

The energy reconstruction algorithm then identifies clusters starting from a central crystal (seed) with an energy deposit of at least 139.5 MeV (or from the most energetic of a pair of adjacent crystals with at least 46.5 MeV each), and adding all the channels above the clustering threshold (18.5 MeV) belonging to a  $5 \times 5$  matrix of crystals centered on the seed. Contiguous clusters are eventually merged. The final cluster energy is obtained after application of channel-to-channel relative calibration constants and of an absolute energy scale factor, set with data taken with a 120 GeV/ $c$  electron beam [10].

The initial sample of useful CMS triggers is reduced by the combined requirements of a muon at the trigger level, of a single muon track reconstructed by the tracker [8] in the range 5-1000 GeV/ $c$ , and of an energy deposit associated with the track in the lower ECAL barrel, since the muon momentum has to be measured upstream of the energy release in the calorimeter. After these and further quality selections applied to the event sample,  $2.5 \times 10^5$  muons are left.

The measured muon spectrum, after the selections, is shown in Fig. 1(a). The spectrum of energy deposited in crystals is shown in Fig. 1(b). Figure 2 displays the distributions of  $dE/dx$  for muons with momentum below 10 GeV/ $c$ , where collision losses dominate (a), and for muons with momentum above 300 GeV/ $c$ , where sizable radiation losses are expected (b).

## 3. Data analysis and systematic correction

### 3.1. Instrumental effects

The relevant instrumental effects are related to the online data reduction and to the energy reconstruction procedure described in Section 2. The presence of thresholds introduces a bias in energy reconstruction: noise fluctuations above threshold contribute a positive bias, while energy deposits below threshold contribute a negative bias.

When the muon direction is close to the crystal axis (angle between muon and crystal axis  $\lesssim 0.1$  radians), the condition for SR is met in the majority of cases. The main positive bias then arises from the probability of noise fluctuation above the clustering threshold. A 14.7 MeV bias is estimated by means of a dedicated analysis of the noise spectrum.

At larger muon angles to the crystal axis, the crystal multiplicity in cluster increases and the average energy deposit per crystal decreases correspondingly. Therefore conditions for ZS readout occur more frequently, with the higher ZS threshold reducing the noise bias. Moreover, the probability that the energy deposited in a single crystal is below clustering threshold increases, thus contributing a negative bias. Bias is then expected to decrease with increasing angles.

<sup>1</sup> Because of the angular distribution of the cosmic ray muon flux and the lower sensitivity of the ECAL end-caps to the energy released by mip muons, only the barrel part of ECAL is used in the present analysis.

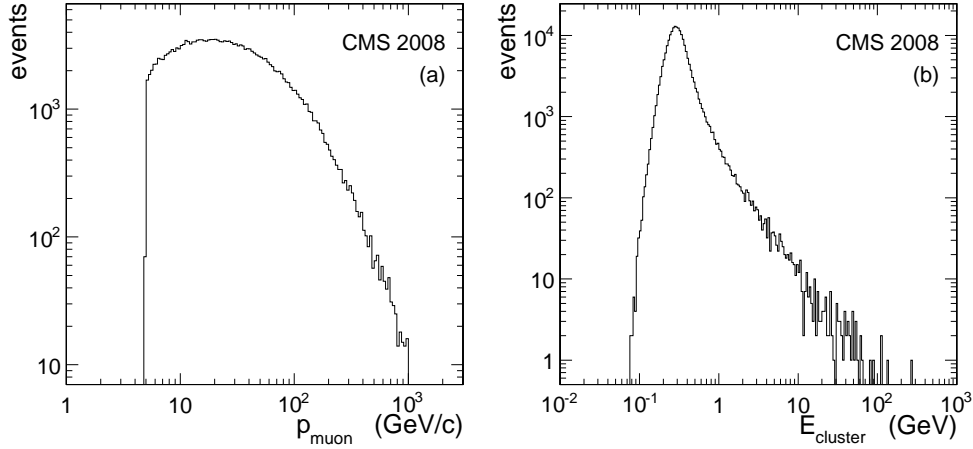


**Figure 1.** (a) Momentum spectrum of the muons passing the selections; (b) spectrum of the reconstructed energy in the lower ECAL hemisphere. A logarithmic binning is used.

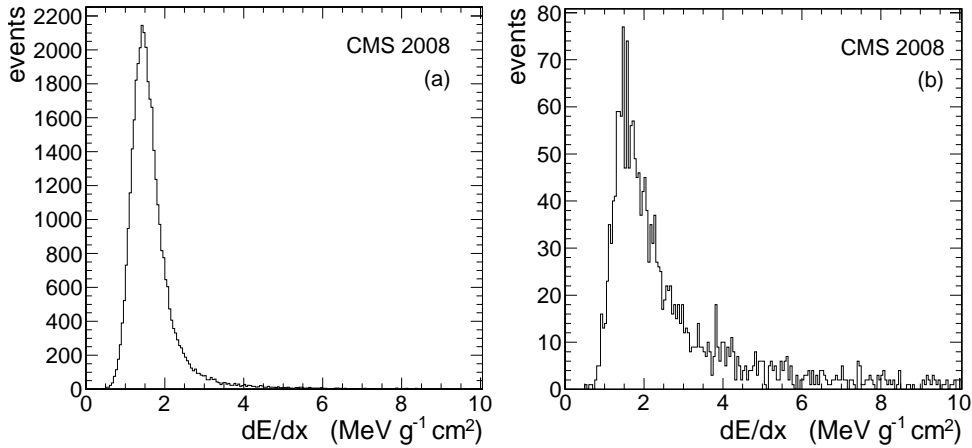


**Figure 2.** Measured distributions of  $dE/dx$  in ECAL; (a) for muon momenta below 10 GeV/ $c$ ; (b) for muon momenta above 300 GeV/ $c$ ; the fraction of events with  $dE/dx > 10 \text{ MeV g}^{-1} \text{ cm}^2$  is  $1.3 \times 10^{-3}$  and  $8 \times 10^{-2}$  in (a) and (b) respectively.

This bias dependence on angle for non-radiating muons is observed in experimental data, as shown in Fig. 3, where the raw measured  $dE/dx$  is displayed versus angle for muons below 10 GeV/ $c$ .

A correction is thus applied to the estimated collision component of the stopping power by applying the following procedure. At small angles, a bias of 14.7 MeV is subtracted. At larger angles, the bias to be subtracted is estimated from a fit to the data shown in Fig. 3. The uncertainty in the evaluation of the 14.7 MeV bias and the statistical uncertainty of the fit contribute to the systematic uncertainty of the bias correction, yielding an overall systematic uncertainty of 3.5 MeV, which corresponds to about 1.2% of the average energy deposited by a low-momentum muon.

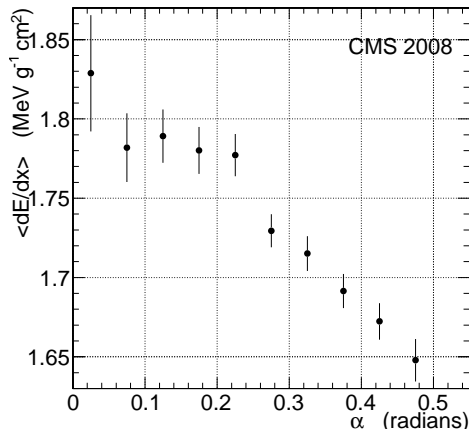


**Figure 3.** Dependence of the raw  $\langle dE/dx \rangle$  on the angle  $\alpha$  between the muon direction and the crystal axis, for muon momentum between 5 and 10 GeV/ $c$ . Vertical bars represent statistical errors.

### 3.2. Containment corrections

An issue to be taken into account is that energy  $\Delta E$  lost by a muon traversing a given volume is in general different from the energy deposited in that same volume, which is the first output of the measurement procedure. For the present experimental setup, it can be shown that there is always a non-negligible flow of energy carried by secondaries leaving the calorimeter volume from the rear crystal face, since secondaries are produced along the entire muon path.

To estimate the difference between energy lost and energy deposited in ECAL, a model based on the Geant4 [11] simulation toolkit, with a simplified description of the detector and materials surrounding it, was developed. Since energy leakage and the effects of upstream and downstream materials on it are quantitatively different for collisions and radiative processes, the two different regimes have been treated separately.

For collisional processes, according to the simulation, the energy carried by secondaries flowing out of the rear detector surface is, on average, 3% of the energy lost in the crystals for a muon with momentum 15 GeV/ $c$ . This represents an upper limit to containment corrections in the low-momentum region, since the rear leakage can be compensated by secondaries produced in upstream material entering the front detector surface. A comparison of the deposits in the upper and lower hemispheres of the ECAL barrel, for muons with momentum between 5 and 10 GeV/ $c$ , shows no difference in  $dE/dx$ , with a sensitivity better than 1% [12]. Given this result, in spite of the asymmetric distribution of the outer and inner material around ECAL, containment correction has been neglected, and 1% systematic uncertainty on the null correction has been assumed for collision losses.

Energy containment corrections for radiative processes have been derived from dedicated simulations as the mean value of two extreme cases: with no material in front of ECAL and with the whole material budget of the tracker concentrated just in front of ECAL, representing the upper and the lower limit to the containment correction. Half of the difference between the results of the two simulations is taken as the associated systematic error. The correction is maximal at 1 TeV/ $c$  and corresponds to  $(28 \pm 5)$ % of the average energy lost, while at 170 GeV/ $c$  it reduces to  $(14.5 \pm 2.5)$ %. Such an uncertainty is small compared to the statistical uncertainty in the measurement of the stopping power in radiative region.

#### 4. Experimental results

In Fig. 4(a), the specific muon energy loss resulting after corrections is compared to expectations as a function of the muon momentum [4]. Fig. 4(b) shows the ratio of experimental measurements to expected values. Two regions are indicated in Fig. 4: the expected 68 % probability central interval (grey shaded area), and the minimum interval corresponding to 68 % probability (region delimited by continuous curves). The reasons for considering both intervals and the procedure adopted for their estimate are summarized below.

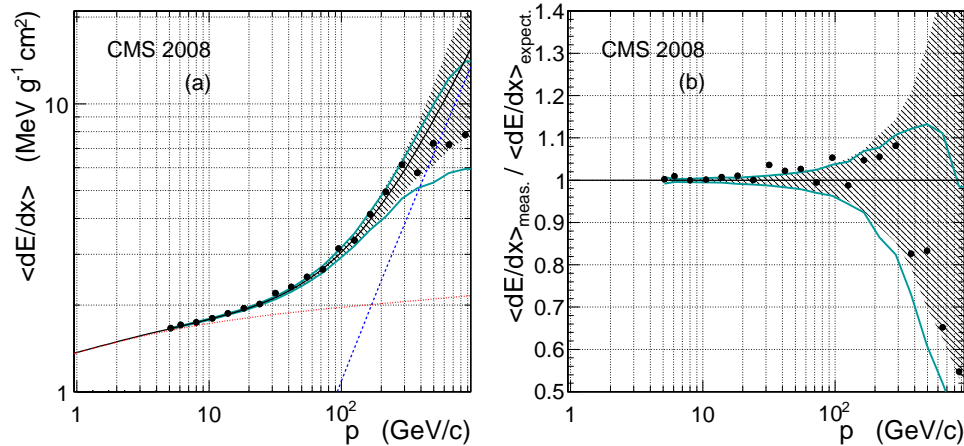


**Figure 4.** (a) Muon stopping power measured in  $\text{PbWO}_4$  (dots) as a function of muon momentum compared to expectations [4] (continuous line). The expected contributions from collision and radiative processes are plotted as well (dotted line and dashed line respectively). (b) Ratio of the measured and the expected values of the muon stopping power, as a function of muon momentum. The shaded grey area indicates the expected 68 % probability central interval, while the continuous curves delimit the minimum interval containing 68 % of the expected results.

Radiative losses are rare events characterized by large energy releases. As a consequence, the probability density functions (pdf) of energy loss for single events are positively skewed distributions, with long tails at high energy. The skewness of the single event pdf increases with increasing muon momentum, owing to the increasing contribution of radiative processes with momentum. At the same time, the number of events per bin in the selected data sample rapidly decreases with momentum for  $p > 50$  GeV/c (Fig. 1(a)). It is thus expected that, due to the combination of these two effects, the pdf of the sample mean of  $dE/dx$  cannot be approximated by a Gaussian in the higher momentum bins. Moreover, when this condition occurs, sample mean and sample variance are highly correlated. It follows that the widely used “experimental error”, namely the sample rms divided by the square root of the sample population, is not a good measure for the consistency of the sample mean with the expected value.

Therefore the uncertainty of the result has been estimated by means of a numerical technique based on the simulation of the expected results with Geant4. Ten thousand pseudo-experiments per momentum bin, each with the same statistics as the actual bin population, were simulated. The expected pdf of the mean was then obtained for each bin as the distribution of the mean values of the stopping power from the different experiments. For each pdf two 68 % probability intervals for the expected result were derived: the central interval, obtained by discarding 16 % of the results on each tail of the pdf, and the interval of minimum width containing 68 % of the results; this last interval always contains the most probable value.

The curve  $(dE/dx)_{meas} = \alpha \left[ \left( \frac{dE}{dx} \right)_{coll} + \beta \times \left( \frac{dE}{dx} \right)_{rad} \right]$ , where *coll* and *rad* label the predicted

energy losses in PbWO<sub>4</sub> due to collisions with atomic electrons and radiative processes respectively [4], is fitted to experimental stopping power data using a binned maximum likelihood and the pdf described above. The parameters  $\alpha$  and  $\beta$  account for the overall normalization of the energy scale and for the relative normalization of radiation and collision losses. With the adopted parameterization the  $\beta$  parameter, from which the critical energy is measured, is independent of the overall energy scale. The fit results in:

$$\alpha = 1.004_{-0.003}^{+0.002} \text{ (stat.)} \pm 0.016 \text{ (syst.)}$$

$$\beta = 1.07_{-0.04}^{+0.05} \text{ (stat.)} \pm 0.6 \text{ (syst.)}.$$

Adding statistical and systematic contributions in quadrature, it may be concluded from the above results that the energy scale is consistent with expectations within a systematic uncertainty of 1.6%, with a 1.2% contribution from the uncertainty on the energy scale dependence on the angle and on the clustering, and a 1.0% contribution from uncertainty in containment corrections. This result is mainly determined by the precision of the measurements in the momentum region below 20 GeV/c, where radiation losses are marginal.

From the fit results, a muon critical energy of  $160_{-6}^{+5} \text{ (stat.)} \pm 8 \text{ (syst.) GeV}$  is obtained, in agreement with the computed value of 169.5 GeV for PbWO<sub>4</sub> [4]. The systematic uncertainty includes a contribution of 4.5 GeV from the uncertainty of the containment corrections, dominated by the limited knowledge of the correction for radiation losses, and a contribution of 6 GeV due to the stability of the result against bias subtraction and event selection.

## 5. Conclusions

The muon stopping power in PbWO<sub>4</sub> has been measured over the momentum range from 5 GeV/c to 1000 GeV/c. In the region corresponding to muon momenta less than 20 GeV/c, where collision losses dominate, the average energy deposited in the crystals is of order 300 MeV. Thus the agreement (to within 1-2%) between the measured stopping power and the calculated values confirms that the energy calibration of the detector, previously determined with 120 GeV/c electrons, remains valid down to the sub-GeV scale.

From a comparison of the rate of collision losses with that of radiative losses, a first experimental determination of the muon critical energy has been obtained. The experimental value  $160_{-6}^{+5} \text{ (stat.)} \pm 8.0 \text{ (syst.) GeV}$  is in agreement with numerical calculations for this material.

## References

- [1] CMS Collaboration 2010 Commissioning of the CMS experiment and the cosmic run at four tesla *JINST* **5** T03001
- [2] Particle Data Group, Amsler C et al. 2008 Review of particle physics *Phys. Lett. B* **667** 1
- [3] Groom Donald E, Mokhov Nikolai V and Striganov Sergei I 2001 Muon stopping power and range tables 10-MeV to 100-TeV *Atom. Data Nucl. Data Tabl.* **78** 183-356
- [4] Particle Data Group 2009 Atomic and Nuclear Properties of Materials, tables for PbWO<sub>4</sub> *web pages at: <http://pdg.lbl.gov/2009/AtomicNuclearProperties/>*
- [5] Ivanov D, Kuraev E A, Schiller A and Serbo V G 1998 Production of e+ e- pairs to all orders in Z alpha for collisions of high-energy muons with heavy nuclei *Phys. Lett. B* **442** 453-8
- [6] CMS Collaboration 2008 The CMS experiment at the CERN LHC *JINST* **3** S08004
- [7] CMS Collaboration 2010 Measurement of the muon stopping power in lead tungstate *JINST* **5** P03007
- [8] CMS Collaboration 2010 Performance of CMS muon reconstruction in cosmic-ray events *JINST* **5** T03022
- [9] Almeida N et al. Data filtering in the readout of the CMS electromagnetic calorimeter 2008 *JINST* **3** P02011
- [10] Adzic P et al. 2008 Intercalibration of the barrel electromagnetic calorimeter of the CMS experiment at start-up *JINST* **3** P10007
- [11] GEANT4 Collaboration, Agostinelli S et al. 2003 GEANT4: A simulation toolkit *Nucl. Instrum. Meth. A* **506** 250-303
- [12] CMS Collaboration 2010 Performance and Operation of the CMS Crystal Electromagnetic Calorimeter *JINST* **5** T03010